Influence of Neutral Beam Injection Direction and Magnetic Axis Position on Fast Ion Distribution Function in Large Helical Device

Evgeny Alexandrovitch VESHCHEV, Tetsuo OZAKI, Tsuguhiro WATANABE, Shigeru SUDO and LHD Experimental Group

National Institute for Fusion Science, Toki, Gifu 509-5292, Japan

(Received 7 January 2009 / Accepted 2 August 2009)

Effective ion heating and good fast ion confinement are essential for ignition. Therefore the influence of various types of plasma heating on the fast ion distribution function in various magnetic field comfigurations should be studied. To study the distribution of fast ions in LHD plasma, a new Angular Resolved Multi-Sightline Neutral Particle Analyzer (ARMS-NPA) has been developed. It scans plasma by 20 sightlines and can provide detailed information about angular and radial distribution of fast particles. In this paper, the influence of co- and counter- neutral beam injection (NBI) on angular distribution of the suprathermal particle tail is shown. Measurements were made for different directions of magnetic field in inward- ($R_{\rm ax}$ = 3.6 m) and outward-shifted ($R_{\rm ax}$ = 3.9 m) magnetic axis position. The suprathermal ion tail angular distribution during co- and counter-NBI was measured for different magnetic field strengths in the current work. The simulation results of fast particle orbits are shown as well to explain the experimental results.

Keywords: fast ion heating, neutral particle, angle resolved measurement, fast particle flux simulation, diagnostic, fast particle orbit, energy resolved measurement, angular distribution function, ion distribution.

DOI: 10.1585/pfr.5.S1024

1. Introduction

Fast ion distribution in a plasma may change significantly under various plasma heating mechanisms with different magnetic field configurations and plasma parameters. Therefore, as effective ion heating and good fast ion confinement are essential for ignition, the fast ion distribution function should be studied properly. For this purpose, numerous diagnostic tools have been developed on modern fusion devices and on the Large Helical Device (LHD) in particular. LHD plasma has a very complex 3D shape that complicates diagnostics and the investigations of the fast particle distribution function.

One recently developed tool is the Angular Resolved Multi-Sightline Neutral Particle Analyzer (ARMS-NPA), which scans plasma by 20 sightlines and is currently being upgraded to scan up to 40 sightlines [1–3]. Among NPAs previously used on the LHD for angular resolved measurements of fast particles, only one had had multiple sightlines, the Silicon Detector based NPA (SD-NPA), with 6 scanning chords [4]. However, the angular resolution of the SD-NPA was not sufficient for in-depth investigations of fast particle angular distribution in a single plasma discharge and for studying of fast particle loss-cone regions in helical plasmas which were predicted theoretically before.

The key feature and unique advantage of the ARMS-NPA is the potential to make detailed time-, angular-, and energy-resolved measurements of fast particle distributions in plasmas in a single plasma discharge.

author's e-mail: Evgeny.Veshchev@iter.org

The first experimental results demonstrated the possible existence of a loss-cone in LHD plasma [3]. At the same time, as comparisons of the fast particle population in plasmas shifted in and outside of the major radius are important in suprathurmal ion confinement studies, investigation of fast particle angular distribution has been started in inward-shifted ($R_{\rm ax}$ = 3.6 m) and outward-shifted ($R_{\rm ax}$ = 3.9 m) magnetic axis position configurations in [3]. As neutral beam injection (NBI) is widely used for fast particle heating and is considered to be a heating mechanism in future fusion devices as well, it is important to study how the direction of NB particles influences fast ion distribution under different plasma conditions and different magnetic axis positions.

In this paper experimental results of fast particle angular distribution obtained by the ARMS-NPA are shown for inward-shifted ($R_{\rm ax}$ = 3.6 m) and outward-shifted ($R_{\rm ax}$ = 3.9 m) magnetic axis positions for co- and counter-injected NB for every case of magnetic axis position. Experimental results are compared with theoretical predictions based on fast ion orbit calculations.

2. Experimental Setup

The position of the ARMS-NPA on the LHD versus NB injectors and ion cyclotron resonance frequency (ICRF) antennas is shown in Fig. 1. To investigate the influence of NBI direction on the angular distribution of fast particles, NBI#1 was used with an energy of injected parti-

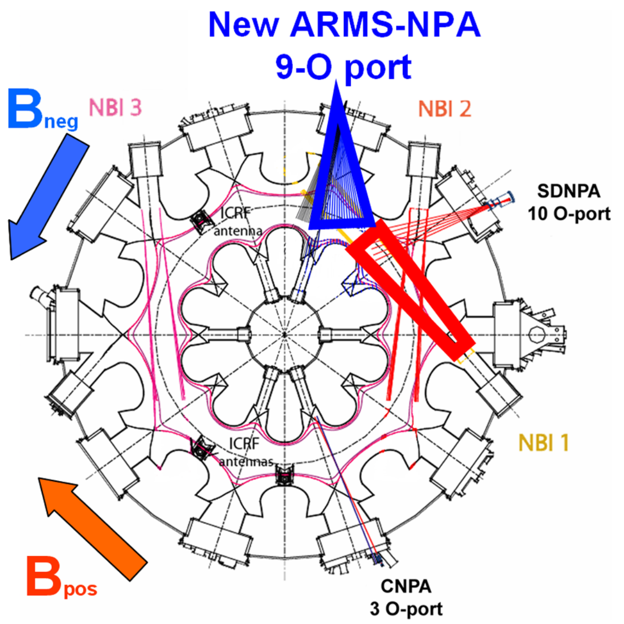

Fig. 1 ARMS-NPA location on LHD (blue) versus NBI#1 (red).

cles equal to 180 keV. When the magnetic field is positive (marked by orange in Fig. 1), NBI#1 serves as a counter-injector, and when it is negative (marked by blue in Fig. 1), NBI#1 serves as a co-injector.

3. Experimental Results

Experimental angular-resolved fast particle spectra are shown in Fig. 2. Spectra in Figs. 2 a) and 2 b) are from co- and counter-injected NBI#1 regimes, respectively, corresponding to an inward-shifted (R_{ax} = 3.6 m) magnetic axis position. Spectra in Figs. 2 c) and 2 d) are from co- and counter-injected NBI#1 regimes, respectively, corresponding to an outward-shifted (R_{ax} = 3.9 m) magnetic axis position. The colored scale units of every picture correspond to ln[$\Gamma(E)$], where $\Gamma(E)$ [counts] is the flux of fast particles detected by the ARMS-NPA.

To demonstrate the influence of magnetic axis shift and the effect of NBI direction on the fast ion angular distribution, discharges with similar plasma parameters were selected for analysis. All measurements were made in low-density regimes ($n_e < 1 \times 10^{19}\,\mathrm{m^{-3}}$) with temperatures T_e = 1.5-2.0 keV. The slowing down time is about

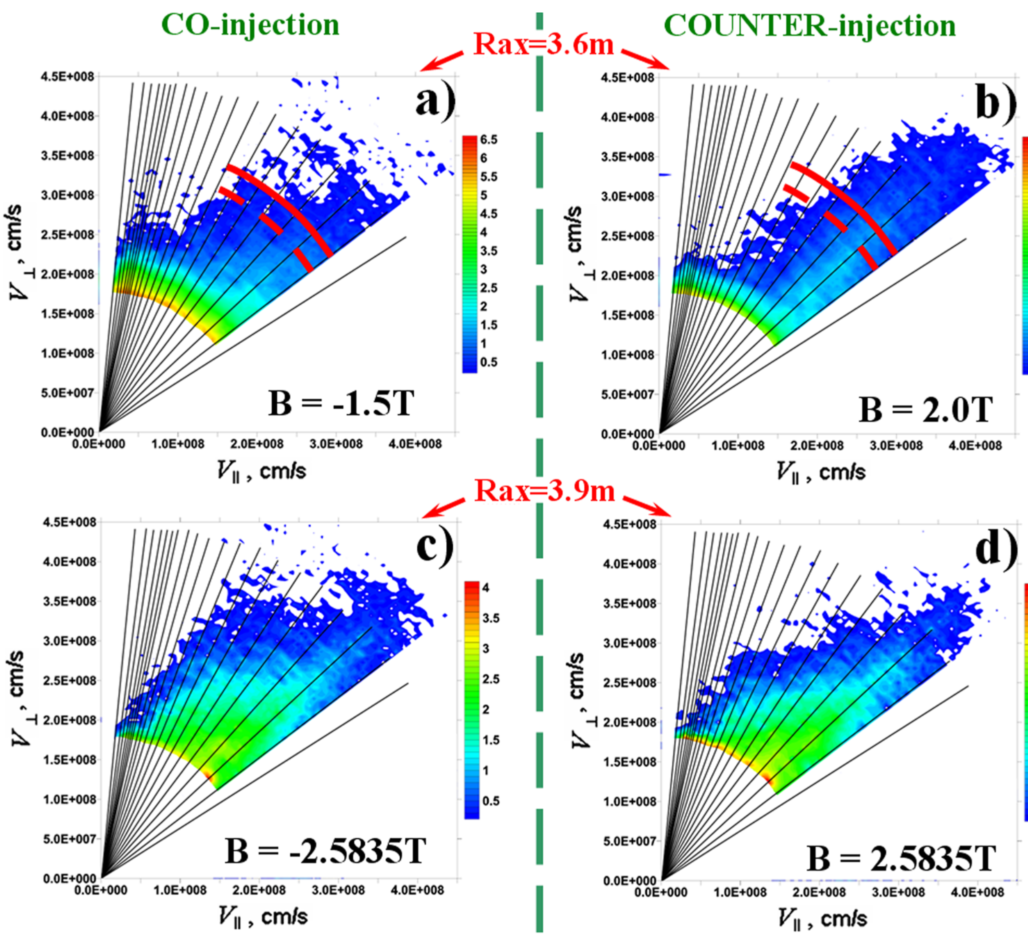

Fig. 2 Comparison of experimental fast particle angular distributions in co- and counter-injected NBI#1 regimes for R_{ax} = 3.6 m and R_{ax} = 3.9 m magnetic axis positions.

310 ms for R_{ax} = 3.9 m for both co-and counter injection; for R_{ax} = 3.6 m, it is 350 ms for co- and 600 ms for counter -injection.

3.1 Magnetic axis shift effect

To evaluate the magnetic axis shift effect on the fast ion angular distribution let's compare spectra obtained in the NBI#1 co-injected regimes with inward (R_{ax} = 3.6 m) and outward (R_{ax} = 3.9 m) magnetic axis positions, *i.e.* compare Fig. 2 a) with Fig. 2 c). For the case of NBI#1 counter-injection let's compare Fig. 2 b) with Fig. 2 d), corresponding to inward (R_{ax} = 3.6 m) and outward (R_{ax} = 3.9 m) magnetic axis positions. These comparisons show that although total flux has been reduced in regimes with outward-shifted magnetic axis (colored scale limit is equal to 4 for R_{ax} = 3.9 m and 6.5 for R_{ax} = 3.6 m), the high-energy tails from NBI#1 in the outward-shifted magnetic axis configuration are wider than those in the inward-shifted magnetic axis configuration.

The probable reason for this difference in fast particle angular distribution for inward- and outward-shifted magnetic axis configurations is a different deposition location of NB particles. Figs. 3 a) and 3 b) illustrate a top view of the LHD chamber and NB axis position (blue line) versus plasma column axis position (red line) for R_{ax} = 3.6 m and R_{ax} = 3.9 m, respectively. The figure shows that for R_{ax} = 3.6 m (Fig. 3 a), the NBI axis doesn't intersect the magnetic axis, but it does intersect it for R_{ax} = 3.9 m (Fig. 3 b).

On the other hand, the magnetic field strength at the axis is larger for R_{ax} = 3.9 m (2.6 T versus 2 T for R_{ax} = 3.6 m). To confirm whether the difference in fast particle angular distribution has appeared due to the magnetic axis shift effect (which changes the NB particle deposition location) or due to increased magnetic field strength, the dependence of fast ion angular distribution on magnetic field strength has been measured for R_{ax} = 3.6 m. The magnetic field strength was varied from −0.75 T to −2.811 T. The results are shown in Fig. 4. It shows the angular distribution of fast particles with energies of 65-70 keV [as marked, for example, on Figs. 2 a) and 2b) by red arcs]. Black circles in Fig. 4 correspond to the positive magnetic field direction and thus, to counter-injected NBI#1. All other colored dots correspond to the negative magnetic field direction and co-injected NBI#1. Black circles and colored dots, except for blue dots, correspond to magnetic axis position at R_{ax} = 3.6 m; blue dots correspond to a slightly outward-shifted magnetic axis position at R_{ax} = 3.65 m.

Fig. 4 shows that although the flux of fast particles increases with increasing magnetic field strength (for the case of negative magnetic field), the angular range of the suprathermal ion tail remains the same (35°-67°) for the case of negative magnetic field and a magnetic axis position at R_{ax} = 3.6 m. However, the slight outward shift of the magnetic axis (R_{ax} = 3.65 m), together with increasing magnetic field strength (B = −2.811 T), leads to broadening of the angular distribution (35°-80°) and increases the

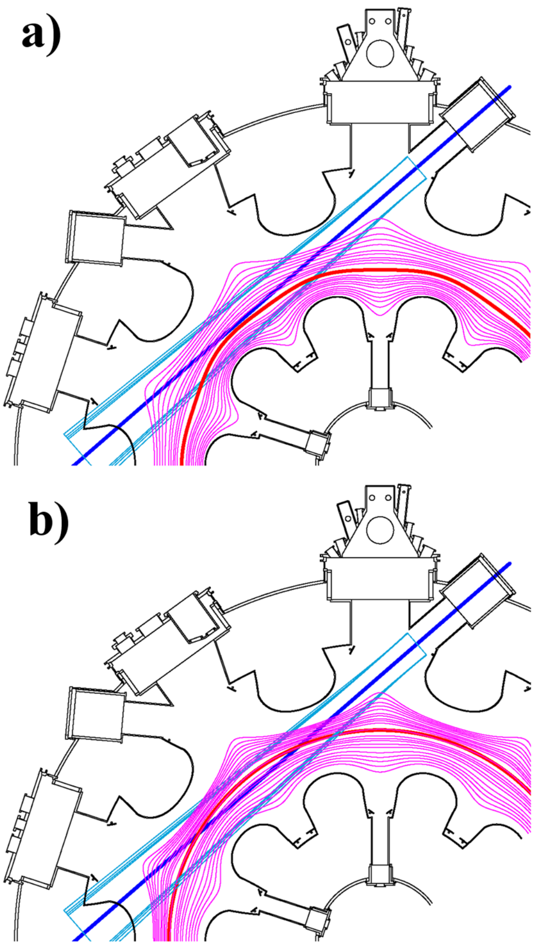

Fig. 3 Top view of LHD chamber. a) R_{ax} = 3.6 m. b) R_{ax} = 3.9 m. Blue line – NBI axis. Red line – magnetic axis.

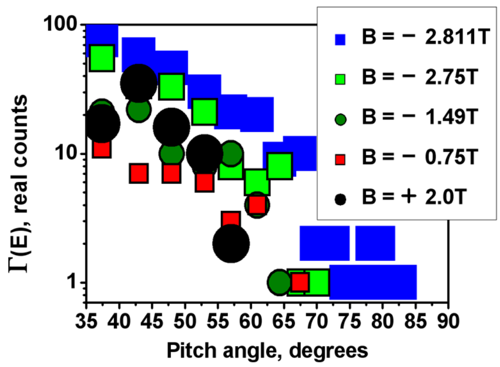

Fig. 4 Angular distribution of high-energy tail particles from NBI#1 (particle energies are in the range of 65-70 keV). Blue squares correspond to the R_{ax} = 3.65 m magnetic axis position. All other dots correspond to R_{ax} = 3.6 m. Black dots correspond to positive magnetic field direction and thus to counter-injected NBI#1; all other dots correspond to negative magnetic field and thus to co-injected NBI#1.

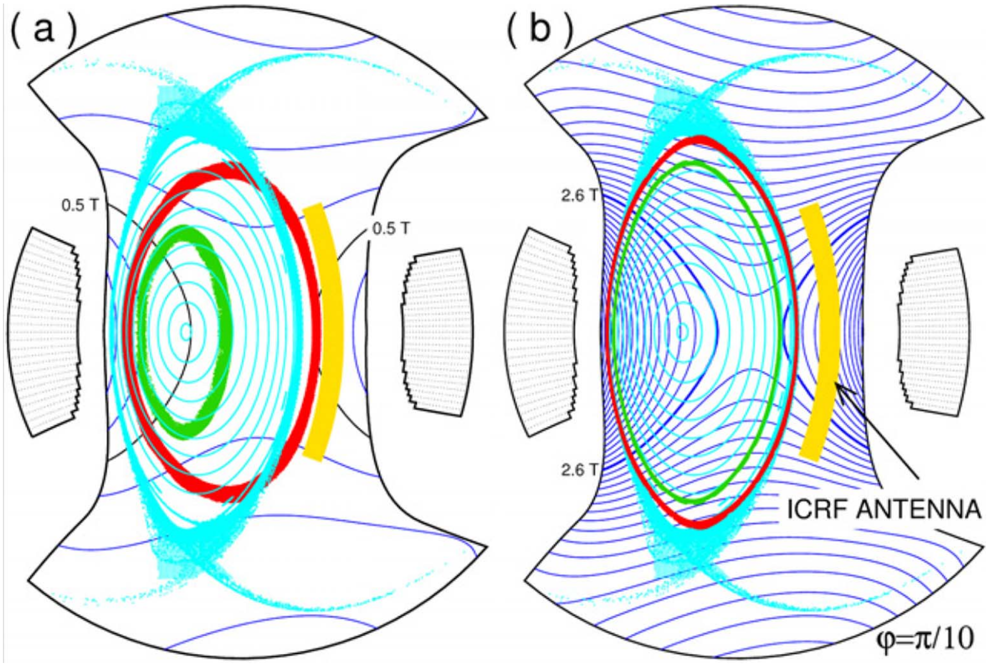

Fig. 5 Relations between the magnetic surface, outermost drift surfaces, and magnetic field intensity are shown by Poincare plots at the poloidal cross section of $\varphi = \pi/10$. Red (green) dots show the outermost drift surface of co-NBI (counter-NBI) particles with $E = 180$ keV. Cyan dots show the structure of lines of force. Position of magnetic axis is inward shifted ($R_{ax} = 3.6$ m). (a) Low magnetic field case ($B_{ax} = 0.5$ T). (b) Standard magnetic field case ($B_{ax} = 2.75$ T).

fast particle population.

3.2 Neutral beam injection direction effect

To evaluate the effect of the NBI direction on the fast ion angular distribution let's compare spectra obtained in co- and counter- regimes for inward ($R_{ax} = 3.6$ m) magnetic axis position, *i.e*. compare Fig. 2 a) with Fig. 2 b); and spectra obtained in co- and counter- regimes for outward ($R_{ax} = 3.9$ m) magnetic axis position, *i.e*. compare Fig. 2 c) with Fig. 2 d). These comparisons show that angular distribution of the high-energy tail from NBI#1 is wider during co-injection for both outward and inward magnetic axis positions.

Fig. 4 clearly shows that the fast particle angular distribution when $B = 2$ T is narrower than those for the case of negative magnetic field, and thus co-injected NBI#1, in the whole range of scanned magnetic field strengths from -0.75 T to -2.811 T.

Therefore, from experimental results it may be concluded that a co-injected NB is more effective than a counter-injected NB for fast ion heating in the LHD.

In addition, the deposition location of NB particles is very important for creating a broader angular distribution of high-energy particle tail from an NB in plasma.

Thus, the outward-shifted magnetic axis configuration with a co-injected NBI (in our case it is $R_{ax} = 3.9$ m, $B = -2.5835$ T, and the use of NBI#1) is the most appropriate for broad heating of fast ions by a tangential NBI in LHD plasma.

3.3 Simulation results

The obtained experimental results can be explained by fast particle orbit simulation results, which predicted that co-injection is more favorable for fast ion heating than counter-injection on the LHD [5]. These simulation results from manuscript [5] can be seen in Fig. 5, which shows the outermost drift surfaces of co-injected (red) and counter-injected (green) NB particles with $E = 180$ keV. The magnetic axis radius is $R_{ax} = 3.6$ m for both cases, and the magnetic field strength at the axes is $B = 0.5$ T for Fig. 5 a) and $B = 2.75$ T for Fig. 5 b).

Fig. 5 b) shows that in the typical LHD operating range ($B_{ax} = 2.75$ T, $E = 180$ keV), the confinement region of counter-injected NB particles is slightly smaller than the last closed flux surface (LCFS), and the confinement region of co-injected NB particles reaches the boundary of the chaotic field line layer exceeding the LCFS. However, in low magnetic field operation, the effect of the $B \times \nabla B$ drift motion increases. The drift surface of the co-NBI can extend fairly far outside the LCFS, and the drift surface of the counter-NBI is reduced fairly well compared with the LCFS, as shown in Fig. 5 a).

4. Conclusion

The angular distribution of fast ions in plasma has been studied with the ARMS-NPA for different NBI directions with different magnetic axis positions. It has been shown that NBI direction and magnetic axis position can significantly influence fast ion distribution. The inner shift of magnetic axis leads to significant growth of the fast particle population. At the same time, an outward shift leads to broadening of the fast ion angular distribution in comparison to that with an inward-shifted configuration. In addition, the angular distribution is broader for co-injection with both inward and outward magnetic axis positions. Therefore, for more effective heating and better ion confinement, the inward-shifted configuration with a co-injected NBI is required.

Furthermore, adjusting the NBI injection direction may become necessary for the inward-shifted configuration. A comparison of fast particle angular distribution during co-injected NBI in the inward and outward magnetic axis positions shows that the angular distribution is wider for the outward-shifted configuration. Therefore, to broaden the fast ion distribution, the NBI axes should be adjusted and shifted inward to cross the magnetic axis, as in the case of the outward-shifted configuration.

[1] E.A. Veshchev *et al.*, Rev. Sci. Instrum. **77**, 10F129 (2006).
[2] E.A. Veshchev *et al.*, Plasma Fusion Res. **2**, S1073 (2007).
[3] E.A. Veshchev *et al.*, Plasma Fusion Res. **3**, S1035 (2008).
[4] J.F. Lyon *et al.*, Rev. Sci. Instrum. **74**, 1873 (2003).
[5] T. Watanabe *et al.*, Nucl. Fusion **46**, 291 (2006).